Quarkonia production in proton-proton and Pb-Pb collisions with ALICE

Yiping Wang on behalf of the ALICE Collaboration.
Email: e-mail: yiping.wang@cern.ch

[1]State Key Laboratory of Particle Detection and Electronics,
University of Science and Technology of China, Hefei 230026, China

Abstract. Charmonia are a valuable tool to investigate nuclear matter under extreme conditions, and particularly the strongly interacting medium formed in heavy-ion collisions. At the LHC energies, the regeneration process has been found to significantly impact the observed charmonium yields. In particular, the measurement of ψ(2S) production relative to J/ψ in Pb-Pb collisions has a strong discriminating power between different regeneration scenarios. Additionally, the study of quarkonium production in proton–proton (pp) collisions represents the reference for interpreting results obtained in Pb–Pb collisions and it is a key measurement to distinguish among the quarkonium production models in pp and p–Pb. In this contribution, preliminary findings on the ratio of ψ(2S)-to-J/ψ and inclusive J/ψ cross section in pp $\sqrt{s}$ = 13.6 TeV in Run 3, as well as published results about double ratio between Pb-Pb and pp collisions at 5.02 TeV and the inclusive J/ψ yield in pp collisions at $\sqrt{s}$ = 13 TeV and Pb–Pb collisions at $\sqrt{s_{\rm NN}}$ = 5.02 TeV in Run 2 measured by the ALICE Collaboration will be presented and compared with existing model calculations.

1 Introduction

Heavy quarks, specifically charm and beauty quarks, serve as excellent probes for studying the QGP, which is the strongly interacting medium formed in high-energy heavy-ion collisions. These quarks are primarily generated via initial hard partonic scattering processes, which occur earlier than the thermalization of QGP, allowing them to undergo the entire evolution of the QGP. Quarkonium is a bound state of a heavy quark and its corresponding anti-quark. It can act as a sensitive probe to study the properties of the QGP. During the evolution of QGP, the production of quarkonium may be suppressed due to the color screening effect [1] and dynamical dissociation [2]. However, at LHC energies, due to the large heavy quark density, (re-)generation processes [3, 4] can happen, enhancing the production of quarkonium to some extent.

In pp collisions, quarkonia are produced as heavy quark pairs followed by hadronization. The mechanism of quarkonium production involves non-perturbative effects. Measuring quarkonium in pp collisions provides valuable insights to test the QCD based models [5]. Moreover, the production of quarkonium in pp collisions serves as the reference to the study of larger systems like p–Pb and Pb–Pb.

J/ψ and ψ(2S) have different system sizes and binding energies, leading to the difference in their dissociation and (re-)generation processes[3, 6]. Therefore, studying both ψ(2S) and J/ψ can provide important information to test the models including recombination process.

The J/ψ are reconstructed in ALICE [7] through the $e^+e^-$and the $\mu^+\mu^-$decay channels at midrapidity ($|y| < 0.9$) and forward rapidity ($2.5 < y < 4$), respectively. There are precise measurements of J/ψ production at both midrapidity and forward rapidity, and ψ(2S) at forward rapidity [8] during LHC Run 2, providing valuable information in model constrain and understanding of QGP. ALICE has upgraded the detectors during the long shut-down [9], enabling more precise quarkonium measurements. A selection of inclusive charmonium measurements with ALICE in pp and Pb–Pb collisions in both Run 2 and Run 3 will be discussed.

2 Results in pp collisions

The inclusive J/ψ production is measured at both midrapidity and forward rapidity at $\sqrt{s}$ = 13 TeV down to p_T =0 [10, 11]. Figure 1 shows the p_T-differential cross section for midrapidity (left) and forward rapidity (right). The results are described reasonably by several Non Relativistic QCD [12–14] (NRQCD) and Improved Color Evaporation models [15] (ICEM), with Fixed-Order Next-to-Leading-Logarithms approach [16] (FONLL) used to calculate the non-prompt contribution. The results do not allow to distinguish between models due to limited precision of model calculations.

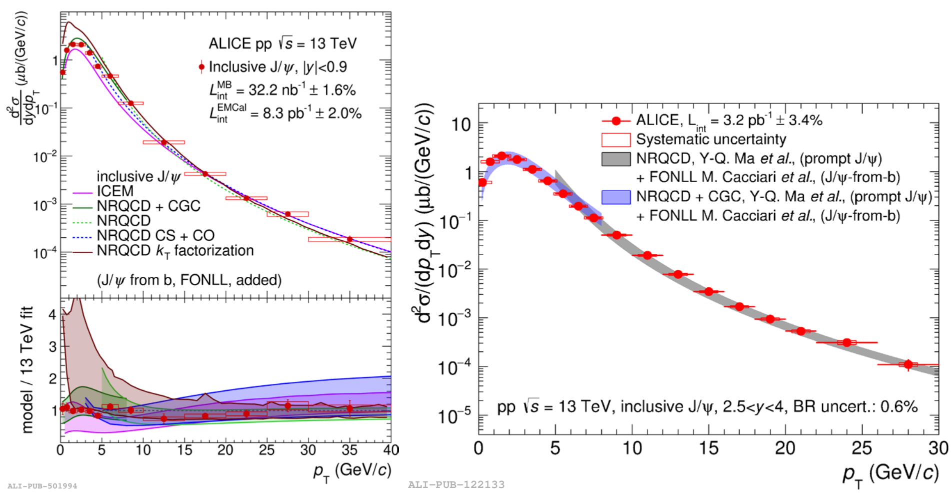

Figure 1. Inclusive J/ψ cross section as a function of p_T in pp collisions at $\sqrt{s}$ = 13 TeV at midrapidity [10] (left), and forward rapidity [11] (right). The results are compared to model calculations from Refs. [12–15]. The non-prompt contributions are calculated using FONLL [16].

In Run 3, the Time Projection Chamber (TPC) has been upgraded with new GEM readout chambers, allowing continuous readout at high luminosity [17]. The preliminary results of inclusive J/ψ cross section measurement at midrapidity can be found in Figure 2. Due to the improvement in statistics, the statistical precision of Run 3 measurement is improved compared with Run 2 results. The data are compared with NRQCD [12, 13, 18] and ICEM [15] calculations. They all give reasonable descriptions.

Thanks to the upgrade in Run 3, ALICE measured ψ(2S) in the central barrel for the first time. The ψ(2S)-to-J/ψ ratio in pp collisions at $\sqrt{s}$ = 13.6 TeV at midrapidity and forward rapidity is displayed in the left and right panels of Figure 3, respectively. The data are compared with several model calculations [12, 13, 15, 18]. ICEM reproduces data well over full p_{T} range, while NRQCD overestimates data, especially at high p_{T}.

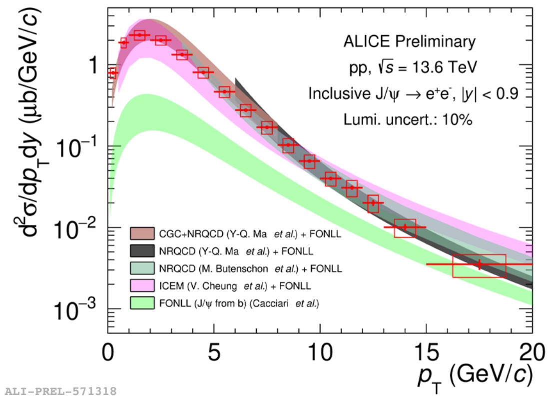

Figure 2. Inclusive J/ψ cross section p_{T} dependence at midrapidity in pp collisions at $\sqrt{s}$ = 13.6 TeV. Results are compared with models in Refs. [12, 13, 15, 18].

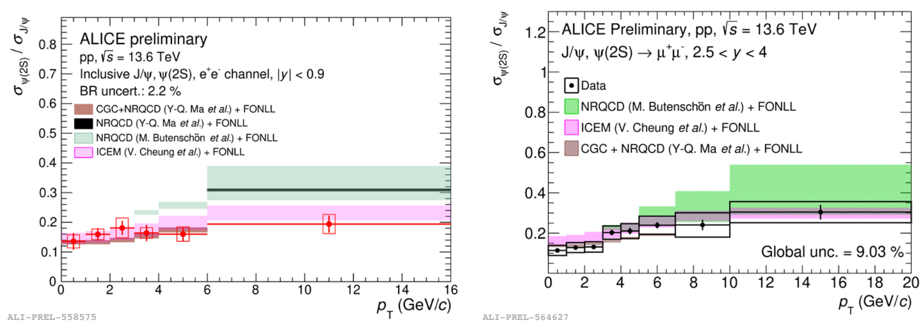

Figure 3. ψ(2S)-to-J/ψ ratio in pp collisions at $\sqrt{s}$ = 13.6 TeV as a function of p_{T} at midrapidity (left) and forward rapidity (right). Results are compared with models from Refs. [12, 13, 15, 18].

3 Results in Pb–Pb collisions

The inclusive J/ψ yield is measured at Pb–Pb $\sqrt{s_{\mathrm{NN}}}$ = 5.02 TeV collisions. The details of the analysis are discussed in Refs. [19]. The p_{T}-differential 0-10% R_{AA} of midrapidity and 0-20% R_{AA} of forward rapidity can be found in the left and the right panel of Figure 4. A clear sign of (re-)generation can be seen at low p_{T}, especially at midrapidity. Two microscopic transport models [20, 21] and statistical hadronization model [22] (SHMc) are used to compare with data. The transport models, which assume charmonium are continuously produced and dissociated during the travel of the cc-bar pairs through the QGP, agree with data over full p_{T} range, while SHMc model, which assumes charmonia are produced at the phase transition according to their thermal weights, shows good agreement only at low $p_{\rm T}$. Energy-loss calculation [23], which is calculated only at high $p_{\rm T}$, can describe the data well, indicating energy loss of partons due to scattering in QGP domains in this region.

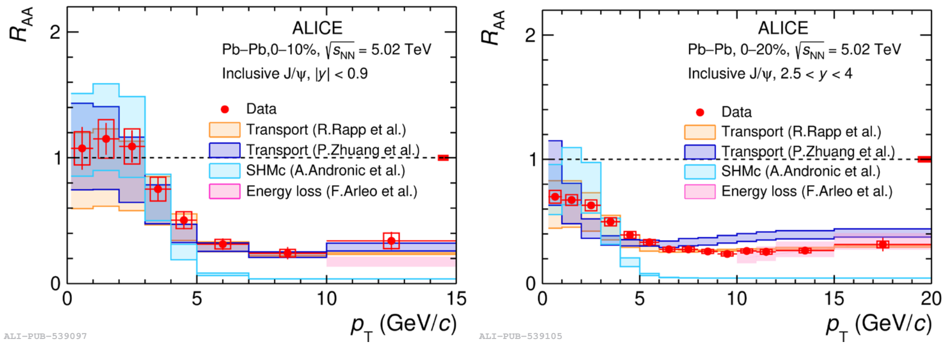

Figure 4. $p_{\rm T}$ dependence of inclusive J/ψ $R_{\rm AA}$ at midrapidity in 0-10% interval (left) and forward rapidity in 0-20% interval. [19] The results are compared with model calculations from Refs. [20–22].

ALICE also reconstructed ψ(2S) using $\mu^{+}\mu^{-}$channel in Pb–Pb at $\sqrt{s_{\rm NN}}$ = 5.02 TeV [8]. The centrality-dependent and $p_{\rm T}$-dependent ψ(2S) $R_{\rm AA}$ are presented in Figure 5. The results are compared with J/ψ $R_{\rm AA}$ [24] and CMS results [25]. In the left panel, ψ(2S) show a stronger suppression compared to J/ψ. SHMc [22] model agrees with J/ψ $R_{\rm AA}$ but underestimates the ψ(2S) $R_{\rm AA}$. TAMU [3] model, which is a transport model assuming continuous generation and dissociation of charmonium, shows a good agreement with data. In the right panel, both ψ(2S) and J/ψ are less suppressed at low $p_{\rm T}$. And TAMU model, which includes the recombination process, reproduces data well within uncertainties, from 0 to 12 GeV/c, indicating the hint of regeneration of ψ(2S) at low $p_{\rm T}$.

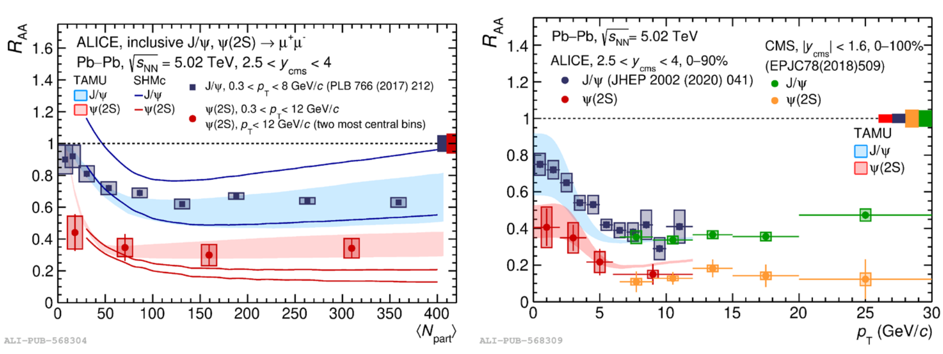

Figure 5. Left: J/ψ and ψ(2S) $R_{\rm AA}$ as a function of centrality [8, 24]. Right: J/ψ and ψ(2S) $R_{\rm AA}$ as a function of $p_{\rm T}$ [8, 24]. Measurements are compared with models in [3, 22] and CMS results [25].

Finally, the ratio and double ratio of ψ(2S)-to-J/ψ in Pb–Pb and pp are computed and presented in Figure 6. SHMc and TAMU predictions calculated at $\sqrt{s_{\rm NN}}$ = 5.02 TeV and NA50 [26] measurement at $\sqrt{s_{\rm NN}}$ = 17.3 GeV are used for comparison with data. Both ratio and double ratio of ψ(2S)-to-J/ψ show no centrality dependence with ALICE. ψ(2S) is suppressed by a factor of ~ 2 with respect to J/ψ, as shown in the bottom panel. TAMU model agrees with data in all centrality intervals, while SHMc model underestimates data.

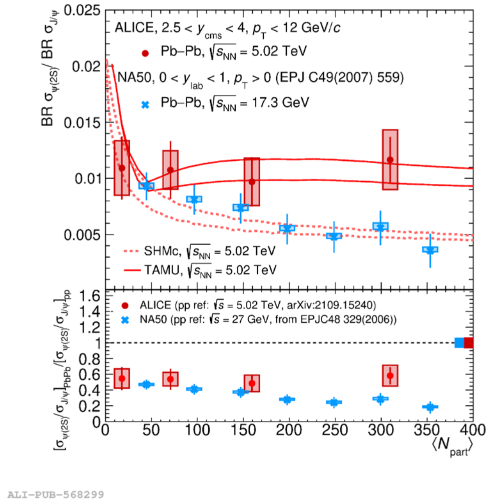

Figure 6. Top: Ratio of ψ(2S) to J/ψ in Pb–Pb $\sqrt{s_{\rm NN}}$ = 5.02 TeV with ALICE [8] and Pb–Pb $\sqrt{s_{\rm NN}}$ = 17.3 GeV with NA50 [26]. Results are compared with [3, 22]. Bottom: double ratio of ψ(2S) to J/ψ in Pb–Pb and pp with ALICE and NA50.

4 Summary

In this contribution, measurements of charmonium production in pp and Pb–Pb collisions with ALICE are presented. In Run 2, there are precise measurements of J/ψ in both pp and Pb–Pb. The existing results show a clear sign of (re-)generation of charmonium in low $p_{\rm T}$ range at LHC energies, especially at midrapidity [19]. Double ratio of ψ(2S)-to-J/ψ between Pb–Pb and pp is measured at forward rapidity, showing a hint of recombination of ψ(2S) [8]. In Run 3, the improved statistics have enabled more precise measurement of J/ψ cross section and the measurement of ψ(2S) at midrapidity. The preliminary results are promising, and more physics results are expected in the future.

5 Acknowledgement

The author is supported in part by the National Key R&D Program of China under Grant No. 2018YFE0104900, the NSFC under grant No. 12475146.

References

[1] T. Matsui, H. Satz, Phys. Lett. B **178**, 416 (1986).
[2] A. Rothkopf, Phys. Rept. **858**, 1 (2020), 1912.02253. 10.1016/j.physrep.2020.02.006
[3] X. Du, R. Rapp, Nucl. Phys A **943**, 147 (2015).
[4] P. Braun-Munzinger, J. Stachel, Nature **448**, 302–309 (2007).
[5] A. Andronic, et al., Eur. Phys. J. C **76**, 107 (2016).
[6] S. Digal, P. Petreczky, H. Satz, Phys. Rev. D **64**, 094015 (2001).
[7] J. Adam et al., (ALICE Collaboration), International Journal of Modern Phys. A **29**, 1430044 (2014).

[8] S. Acharya (ALICE Collaboration), $\psi(2S)$ Suppression in Pb-Pb collisions at the LHC, Phys. Rev. Lett. **132**, 042301 (2024). 10.1103/PhysRevLett.132.042301
[9] ALICE Collaboration, ALICE upgrades during the LHC Long Shutdown 2, Journal of Instrumentation **19**, P05062 (2024). 10.1088/1748-0221/19/05/p05062
[10] ALICE Collaboration, Inclusive J/ψ production at midrapidity in pp collisions at $\sqrt{s}$ = 13 TeV, The European Physical Journal C **81** (2021). 10.1140/epjc/s10052-021-09873-4
[11] ALICE Collaboration, Energy dependence of forward-rapidity J/ψ and ψ(2S) production in pp collisions at the LHC, The European Physical Journal C **77** (2017). 10.1140/epjc/s10052-017-4940-4
[12] Y.Q. Ma, K. Wang, K.T. Chao, $J/\psi(\psi')$ Production at the Tevatron and LHC at $O(\alpha_s^4 v^4)$ in Nonrelativistic QCD, Physical Review Letters **106** (2011). 10.1103/physrevlett.106.042002
[13] M. Butenschön, B.A. Kniehl, Reconciling J/ψ Production at HERA, RHIC, Tevatron, and LHC with Nonrelativistic QCD Factorization at Next-to-Leading Order, Phys. Rev. Lett. **106**, 022003 (2011). 10.1103/PhysRevLett.106.022003
[14] A.V. Lipatov, M.A. Malyshev, S.P. Baranov, Particle event generator: a simple-in-use system PEGASUS version 1.0, The European Physical Journal C **80** (2020). 10.1140/epjc/s10052-020-7898-6
[15] Production and polarization of prompt J/ψ in the improved color evaporation model using the k_T-factorization approach, author = Cheung, Vincent and Vogt, Ramona, Phys. Rev. D **98**, 114029 (2018). 10.1103/PhysRevD.98.114029
[16] M. Cacciari, S. Frixione, N. Houdeau, M.L. Mangano, P. Nason, G. Ridolfi, Theoretical predictions for charm and bottom production at the LHC, Journal of High Energy Physics **2012** (2012). 10.1007/jhep10(2012)137
[17] C. Lippmann (ALICE), Upgrade of the ALICE Time Projection Chamber (2014).
[18] Y.Q. Ma, R. Venugopalan, Phys. Rev. Lett. **113**, 192301 (2014).
[19] ALICE Collaboration, Measurements of inclusive J/ψ production at midrapidity and forward rapidity in Pb–Pb collisions at $\sqrt{s_{\rm NN}}$ = 5.02 TeV, Physics Letters B **849**, 138451 (2024). https://doi.org/10.1016/j.physletb.2024.138451
[20] K. Zhou et al., Medium effects on charmonium production at ultrarelativistic energies available at the CERN Large Hadron Collider, Phys. Rev. C **89**, 054911 (2014), `1401.5845`. 10.1103/PhysRevC.89.054911
[21] X. Zhao, R. Rapp, Transverse momentum spectra of J/ψ in heavy-ion collisions, Physics Letters B **664**, 253–257 (2008). 10.1016/j.physletb.2008.03.068
[22] A. Andronic et al., Transverse momentum distributions of charmonium states with the statistical hadronization model, Phys. Lett. B **797**, 134836 (2019), `1901.09200`. 10.1016/j.physletb.2019.134836
[23] F. Arleo, Quenching of Hadron Spectra in Heavy Ion Collisions at the LHC, Phys. Rev. Lett. **119**, 062302 (2017), `1703.10852`. 10.1103/PhysRevLett.119.062302
[24] A. Collaboration, J/ψ suppression at forward rapidity in Pb–Pb collisions at $\sqrt{s_{\rm NN}}$ = 5.02 TeV, Physics Letters B **766**, 212–224 (2017). 10.1016/j.physletb.2016.12.064
[25] A.M. Sirunyan et al. (CMS), Measurement of prompt and nonprompt charmonium suppression in PbPb collisions at 5.02 TeV, Eur. Phys. J. C **78**, 509 (2018), [Erratum: Eur.Phys.J.C 83, 145 (2023)], `1712.08959`. 10.1140/epjc/s10052-018-5950-6
[26] NA50 Collaboration, J/ψ and ψ' production and their normal nuclear absorption in proton-nucleus collisions at 400GeV, The European Physical Journal C **48**, 329–341 (2006). 10.1140/epjc/s10052-006-0079-4